Comparison of immittance spectroscopy analyses of ultra-pure and "pure" water in the lower frequency regime

J. Ross Macdonald *

Department of Physics and Astronomy, University of North Carolina, Chapel Hill, NC 27599

ABSTRACT

Two different analyses of impedance data obtained from ultra-pure water allowed to equilibrate with the atmosphere have recently appeared. They both thus show much smaller low-frequency resistances than does ultra-pure water. Different fitting models were used in these analyses and led to appreciably different parameter estimates from their data fits. Their two "pure" water experimental data sets are here analyzed with a Poisson-Nernst-Planck model that incorporates the possibility of dissociation of a neutral species to positive and negative charges of arbitrary mobilities, anomalous diffusion in the interface region, and reaction of mobile ions at the electrodes. Complex-nonlinear-least-squares fitting of these data sets with either charges of a single sign mobile or with those of both signs mobile showed that the one-mobile choice was far superior to the two-mobile one. These results were compared both with newly calculated theoretical ultra-pure water immittance ones and with the results obtained in the earlier two papers, where different Poisson-Nernst-Planck-related fitting models were employed. Both involved the restrictive assumptions of full dissociation and two-mobile behavior with equal mobilities of the positive and negative charges. The dominant mobile charge species present in the equilibrated "pure" water data sets (protons for the ultra-pure water), involved mobile impurity ions, possibly oxygen ones. The Poisson-Nernst-Planck model used here is simpler than the other models, and it led to better fits of the data sets and to more physically significant parameter estimates than did the earlier fits.

© 2014 Elsevier Ltd. All rights reserved.

1. Introduction

Water is endemic to life and essential to it since it is a crucial component of biological cells [1]. It is therefore surprising that although its dielectric behavior has been studied in the terahertz frequency region [2], relatively little work on the impedance behavior of pure water in lower frequency regions has been published. Two interesting papers on this subject have recently appeared, however [3,4]. For convenience, they will be identified hereafter by the names of their primary authors, Lenzi and Duarte, respectively. Both used Milli-Q deionized water for their measurements, and the Duarte one quoted the measured resistivity of their sample of such water as 18 Mohm-cm (55 nS/cm), appropriate for ultra-pure water at 25 °C.

Although results for several different situations were provided in papers [3,4], their only common one involved steel electrodes, an electrode area of 3.14 cm^2, and an electrode separation of 1 mm. Both data sets were presumably measured at room temperature,

though not so stated. The measurement temperature value is needed in some of the subsequent fits and calculations, and it will be here assumed to be 25 °C. Only data and fit results were provided by the authors at the impedance level, but here their comparable results are plotted at both the impedance and admittance levels in Fig. 1-a and -b.

The common electrode area/separation length ratio, $CC \equiv A/L$, was 31.4 cm, and this number and its $\log_{10}$ value of about 1.5, may be used to transform the present impedance data of Fig. 1 to specific form. We see that it then only leads to a Duarte mid-range specific real-part resistivity value of about 1.8 Mohm-cm, considerably less than the ultra-pure value quoted above, and the corresponding Lenzi value is appreciably smaller, as discussed later. On request, the authors of these papers kindly sent me their impedance-level data sets. Because of the importance of the subject and because the fits and analyses in these two papers are incomplete, the present work involves more detailed and accurate impedance-spectroscopy (IS) model fits and analyses of these data sets, and their results are compared as well to theoretical IS responses calculated from known numerical parameters for ultra-pure water. Lists and definitions of all acronyms and symbols used herein are included below.

* Tel.: +919 967 5005.
   E-mail address: macd@email.unc.edu

Acronyms and abbreviations

CC	The quotient, A/L, of electrode area, A, and electrode separation, L
CJ	Chang-Jaffé
CJPNP	Poisson-Nernst-Planck model with CJ boundary conditions
CJPNPA	Poisson-Nernst-Planck anomalous-diffusion model with C-J boundary conditions
CNLS	Complex nonlinear least squares
CPE	Constant-phase distributed circuit element (DCE)
GEPNPA	A composite PNP model used in the work of Ref.3 and earlier publications by E. K. Lenzi
GR	Generation-recombination; parameter $k_{gr} \equiv k_g/k_r$; see Section 2.1
IS	Immittance or impedance spectroscopy. Immittance denotes all or any of the four levels of raw data (or specific data): impedance, Z; electrical modulus, M; admittance, Y; and complex dielectric constant, ε.
LEVMW	Windows version of the original CNLS fitting program LEVM
PDRMS	The root-mean-square value of the relative standard deviations of the estimated values of the free model parameters of a CNLS fit
PNP	Poisson-Nernst-Planck ordinary-diffusion model; see Ref. 15.
PNPA	Poisson-Nernst-Planck anomalous-diffusion model

Definition of principal parameters

A	Area in cm^2 of each of the identical electrodes
CELCAP	$(A/L)\,\varepsilon_V$, in Farads
c_0	Concentration of mobile positive and negative charges, in cm^{-3}
C_∞	High-frequency-limiting bulk capacitance of measured material, $(A/L)\,\varepsilon_\infty\varepsilon_V$
D_i	Diffusion coefficients: positive mobile charges, $D_1 = D_p$; negative mobile charges $D_2 = D_n$ (units cm^2/s)
ε_V	The permittivity of vacuum, 8.8542x10^{-14} F/cm
ε_∞	The high-frequency-limiting dielectric constant of the measuring cell material
k_g	Generation rate parameter (units 1/s)
k_i	Chang-Jaffé electrode reaction rates: i=1: positive charge; i=2: negative charge. $k_i \equiv (2D_i/L)\rho_i$, (units cm/s)
k_r	Bimolecular recombination parameter (units cm^3/s)
k_{gr}	k_g/k_r (units cm^{-3})
k_B	Boltzman constant
L	Separation in cm of the identical electrodes
L_{Dj}	Debye length in cm; j=1: one-mobile; j=2: two mobile, $[\varepsilon_\infty k_B T/(je^2 c_0)]^{0.5}$
M_j	$(L/2L_{Dj})$: one- and two-mobile dielectric-ratio dimensionless quantities
N_0	Concentration in cm^{-3} of a neutral species that partly or fully dissociates into positive and negative species of equal concentration
Π_m	$D_2/D_1 \equiv \mu_2/\mu_1$
R_∞	The high-frequency-limiting resistance in ohms of the measuring cell material, in ohms; $(L/A)/[e\,c_0\,(\mu_n + \mu_p)]$
ρ_2	Normalized, dimensionless reaction rate for negative charges; $\rho_2 \equiv (L/2D_2)k_2$, where k_2 is the reaction rate in cm/s. See Eq. (9) for specific adsorption complex form

ρ_∞	Specific high-frequency limiting resistivity: $(A/L)R_\infty$ (ohm-cm)
S_F	Standard deviation of the relative residuals of a CNLS fit
σ_∞	Specific conductivity: $(1/\rho\infty) \equiv (e\mu_n c_0)(1 + \Pi_m^{-1})$ in S/cm
T	Absolute temperature (K)
μ_i	Mobilities: positive mobile charges $\mu_1 = \mu_p$; negative mobile charges $\mu_2 = \mu_n$, in cm^2/Vs
Z_T	Total impedance of a model; often expressed per unit electrode area

Lenzi and Duarte (Refs. 3 and 4) fitted their data sets with different theoretical models (discussed in Sections 2.2.1 and 2.2.2 below) and found less complete and less accurate results than would have been the case had they used the full Poisson-Nernst-Planck (CJPNPA) continuum-diffusion model [5–7]. This composite model involves the ordinary-diffusion PNP one with Chang-Jaffé (CJ) electrode reaction-rate parameters [5,6,8], designated the CJPNP model, and also with the possibility of anomalous rather than ordinary diffusion [5,7], the PNPA model. More information and more specific comparisons can be obtained using the CJPNPA model to fit the two data sets, as discussed in the following sections. The model is available as part of the comprehensive free LEVMW complex-nonlinear-least squares fitting program [9]. It is therefore important to compare the fit results obtained by these authors with full CJPNPA fits of the same sets and, as well, compare with exact immittance results calculated using known ultra-pure water parameters.

Results of immittance spectroscopy (IS) responses and fits of the theoretical and experimental data sets in specific form are therefore described below. The CJPNPA model involves Chang-Jaffé boundary conditions and anomalous diffusion of charged species. Further, the PNP designation used here not only to includes the
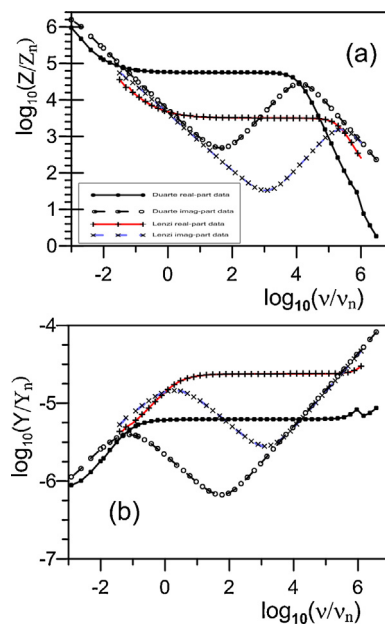

Fig. 1. Comparison of Duarte and Lenzi immittance water data sets: (a) impedance level; (b) admittance level. All Duarte data points are shown but to avoid crowding only every other Lenzi data point is included. Here and elsewhere, $\nu_n \equiv 1$ Hz, $Z_n \equiv 1\,\Omega$, and $Y_n \equiv 1$S.
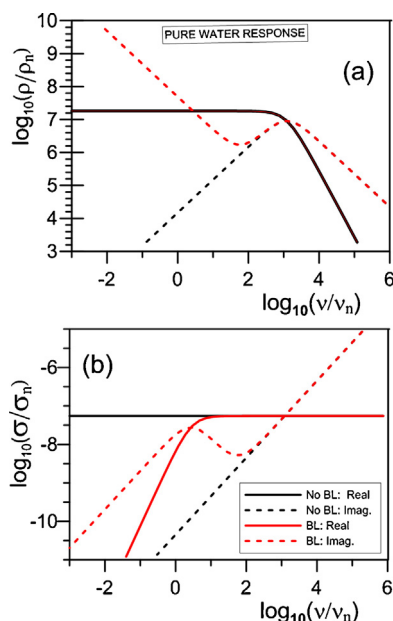
Fig. 2. Ultra-pure water exact no-blocking and full-blocking immittance responses for specific data at (a) the complex resistivity level and (b) the conductivity level. Although there is no difference between the no-blocking and full-blocking response for the real-part resistivity line, as shown here, major differences appear for the rest of the responses. Here $\rho_n \equiv 1\Omega - cm$, and $\sigma_n \equiv 1S/cm$.

PNP behavior dominant in interface regions near electrodes but, for completeness, also the high-frequency-limiting resistive and dielectric parameters ρ_∞ and ε_∞, in specific notation. As shown in Fig. 2b of [5], the resulting circuit diagram involves a resistance involving ρ_∞ in series with the PNP response and the combination in parallel with a capacitance involving ε_∞.

2. Comparison of parameter estimates obtained from model fitting

2.1. Ultra-pure water: theoretical immittance responses

Much information about the parameter values defining ultra-pure water may be obtained by internet searches on such subjects as "water resistivity", "pure and ultra-pure water", and "protonic mobility in water." Protons diffuse through the hydrogen bond network of water and of other hydrogen-bonded liquids by the Grotthuss mechanism [10] involving the cleavage of covalent bonds and tunneling from one water molecule to the next, resulting in excess mobile protons or protonic defects, as described under that title in Wikipedia. There, a value for the resulting proton mobility in water is listed as 3.62×10^{-3} cm^2/Vs. The resistivity of ultrapure water arises from the dissociation of H$^+$ and OH$^-$ ions, very small indeed at 25 °C. As cited in Wikipedia under "Purified water", three types of pure water are roughly defined by their resistivity range, in Mohm-cm, at this temperature: Type 1+ (18.18); Type 2 (>1 to <18); and Type 3 (>0.05 to 1). However, it is stated there that the Type 1+ value is only observed in the presence of monatomic gases and "Completely de-gassed ultra-pure water has conductivity of 1.2×10^{-6} S/cm, whereas upon equilibration to the atmosphere it is 7.5×10^{-7} S/cm due to dissolved CO$_2$ in it."

A full PNP fit of a given data set in specific form involves the PNP response in series with a high-frequency limiting resistivity, ρ_∞, and that combination in parallel with a specific capacitance involving the high-frequency limiting dielectric constant of the material, ε_∞. For the present calculation, I initially assume that the response is fully dominated by mobile protons (the "one-mobile" situation).

At 25 °C and one atmosphere pressure the high-frequency dielectric constant of pure water is about 78.46, the value used here. In order to calculate PNP immittance responses for exact specific data I use the high-frequency ultra-pure water resistivity value of 1.818×10^7 ohm-cm and then determine, using PNP fitting, the protonic concentration, c_0, that leads to its quoted mobility of 3.62×10^{-3} cm^2/Vs. The resulting value was $c_0 = 9.484 x 10^{13}$ cm^{-3}.

Since the concentration of water molecules per cubic centimeter, N_0, is about 3.34×10^{22} cm^{-3}, it is evident that the ultra-pure water dissociation ratio is of the order of a part per billion. Exact response results for no blocking of mobile ions at the electrodes and ordinary rather than anomalous diffusion, the CJPNP model, and for full blocking, the PNP model, are presented in Fig. 2 where all quantities are in cgs units. Comparison of the results of Fig. 1 and Fig. 2 indicate that the experimental data sets of Fig. 1 are closer to full blocking of mobile charge species than to no blocking.

Although fitting of a data set with the PNP model may lead to estimates of the values of both N_0 and c_0 in favorable cases [6], the experimental data of Refs. 3 and 4 require one to either make the assumption of full dissociation of the mobile charge species, leading to the identical estimates of the values of N_0 and c_0, or to use a fixed value of N_0 and allow the PNP program to estimate the k_{gr} ratio of the generation to recombination quantities, k_g and k_r [6]. Here k_g is a generation rate (units 1/s) and k_r is a bimolecular recombination parameter (units cm^3/s). Since the second choice above provides more information, we choose it here, although both approaches yield the same c_0 estimate for a given data set. For the PNP model fits of the present theoretical ultra-pure water data with the fixed value of N_0 cited above, one obtains the c_0 estimate above and a k_{gr} estimate of about 2.692×10^5 cm^{-3}, as listed in row-1 of Table 1 below. Since this value is far smaller than that of N_0, the mobile ion concentration is well approximated by $c_0 \cong (k_{gr}N_0)^{0.5}$ and the dissociation ratio by $(k_{gr}/N_0)^{0.5}$ [6]. The value of c_0 is determined by the data and is independent of N_0 when that quantity is fixed. Therefore doubling the value of N_0, on the assumption that both hydrogens of the water molecule lead to simultaneously mobile protons, produces a halving of the value of k_{gr} and thus properly to halving the value of the dissociation ratio. All the k_{gr} estimates quoted in the rest of this work will, however, be based on the 3.34×10^{22} cm^{-3} value of N_0 since the hydrogen of the OH$^-$ species is strongly bound, leaving only the H$^+$ ion to participate in Grotthuss mobility for ultra-pure water. For less pure water, some other mobile-ion impurity appears to be dominant.

2.2. Fitting results of experimental data of "pure" water

The authors of Refs. 3 and 4, involving IS model fittings of their samples of ultrapure water, did not take actions to maintain its high resistivity by such procedures as degassing and measurement in the presence of a monatomic gas atmosphere, and although their water samples were characterized as pure in these papers, it will be called "pure" here. Thus it is of particular interest to compare their results not only with those for ultrapure water but with full CJP-NPA fits of their two different data sets. The results of such fits and comparisons are summarized in Table 1 and are discussed individually below. Table 1 includes the usual fit-quality parameters (in percentage format) obtained from LEVMW fits, namely 100S$_F$ (a percentage value of the dimensionless quantity S$_F$) and 100PDRMS, where S$_F$ is the relative standard error of the fit residuals and PDRMS is the root-mean-square value of the relative residuals of all free parameters of the fit. These useful quantities, not provided in [3,4], are, however, summaries of the overall goodness of fit, and even more detail is provided here by linear-log plots of the real and imaginary parts of the relative fit residuals vs the logarithm of frequency.

Table 1
Results of LEVMW CNLS proportional–weighting CJPNPA-model one-mobile fits (1 M) of ultra-pure (UPW) and "pure" water data sets in specific form of Duarte (DU) and Lenzi (LE) at the complex conductivity level (rows 1 and 5 and 2 and 6, respectively). Also the results of two-mobile fits (2 M) of the same data sets appear in rows 3 and 7. For easy comparison, the exact ultra-pure-water results of row-1, a PNP or CJPNP model fit, are duplicated in row-5. The "pure"-water-data fits of row 2 and 6 involve the CJPNPA model in series with a resistivity parameter, ρ_s. The previously published 2ME fit results of rows 4 and 8 both include steel electrodes and involve different generalizations of the ordinary CJPNP and CJPNPA models, as described in the text. All parameter values are in cgs units and are appropriate for a temperature of 25 °C. Thus, the units of ρ_∞ and ρ_s are Ω-cm here and that of the Chang-Jaffé parameter electrode-reaction-rate of the mobile ions, k_i, is in cm/s. The letter "F" designates a fixed parameter of a fit.

| #, Data; fit info	$100S_F$ $100PDRMS$	ε_∞	$10^{-4} M_j$	$10^{-6}\,\rho_\infty$	ρ_s	N_0	c_0	k_{gr}	ψ_p	k_i	μ_i	D_i
1 UPW 1M exact data fit	-----	78.46	0.0461	18.18	-----	3.34×10^{22} F	9.48×10^{13}	2.692×10^5	1	0 or ∞	3.62×10^{-3}	9.30×10^{-5}
2 DU 1M fit CJPNPA	1.65 2.89	80.60	2.53	1.77	426	3.34×10^{22} F	2.93×10^{17}	2.57×10^{12}	0.858	5.74×10^{-8}	1.20×10^{-5}	3.09×10^{-7}
3 DU 2M fit CJPNPA	1.81 19.9	80.74	3.63	1.77	429.	3.01×10^{17}	3.01×10^{17}	------	0.857	5.37×10^{-8}	1.17×10^{-5} 2.61×10^{-8}	2.99×10^{-7} 6.69×10^{-10}
4 UPW 2ME fit Ref. 4	-----	-----	-----	-----	-----	1.0×10^{15}	1.0×10^{15}	------	1	?	2.14×10^{-3} 2.14×10^{-9}	5.50×10^{-5} 5.50×10^{-11}
5 UPW 1M exact data fit	-----	78.46	0.0461	18.18	-----	3.34×10^{22} F	9.48×10^{13}	2.692×10^5	1	0 or ∞	3.62×10^{-3}	9.30×10^{-5}
6 LE 1M fit CJPNPA	1.42 2.50	78.16	1.08	0.097	3085	3.34×10^{22} F	5.20×10^{16}	8.08×10^{10}	0.783	4.96×10^{-6}	1.24×10^{-3}	3.19×10^{-5}
7 LE 2M fit CJPNPA	1.08 9.12	77.73	1.29	0.097	3019	3.70×10^{16}	3.70×10^{16}	------	0.795	7.96×10^{-6}	1.65×10^{-5} 5.05×10^{-5}	4.36×10^{-5} 1.30×10^{-6}
8 LE 2ME fit Ref. 3	----- -----	76	-----	-----	-----	2.26×10^{15}	2.26×10^{15}	------	?	7.3×10^{-4}?	5.92×10^{-5}	1.52×10^{-6}
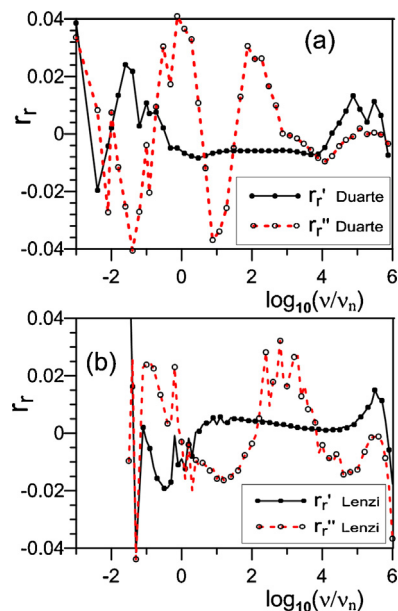
Fig. 3. Comparison of the real and imaginary parts of the relative residuals obtained from resistivity-level CJPNPA model fits of the Duarte (Fig. 3a) and Lenzi (Fig. 3b) water data summarized in rows 2 and 6, respectively, of Table 1.

Since the present log-log CJPNPA fits of the data sets in specific form were better than those presented in Refs. 3 and 4 and they show little or no observable differences from the data, point-by-point residual responses are here provided by plots of the relative residuals. For a CNLS fit, the relative residuals, $r_r \equiv r_r' + ir_r''$, are defined at the resistivity level for each measured frequency as (data value – fit value)/(fit value). Fig. 3 compares the relative residuals obtained from the CJPNPA-model fits of the Duarte and Lenzi experimental data sets. Although their overall fit-quality values in Table 1 are comparable, it appears that the magnitudes of the Lenzi ones are generally smaller. However, not shown is the height of the lowest-frequency Lenzi real-part value of about 0.07, beyond the scale of Fig. 3-b. When this data point was not included in the fit, the resulting estimated parameter values were little changed except for the k_i reaction-rate one, which was then somewhat smaller.

The three different fitting models used in obtaining the parameter estimates listed in Table 1 are both similar and different but a main aim of all three was to fit and explain the low-frequency rise in the real part of the impedance, shown here in Fig. 1 and beginning at a frequency of about 1 Hz or below. As already mentioned, the CJPNPA model [5–7] involves ordinary PNP response modified to take account of anomalous diffusion with a single fractional constant-phase-like exponent (CPE), ψ_p, with $0 < \psi_p \leq 1$ or 2, and electrode-reaction parameters, k_1 and k_2 (designated k_i, with i = 1 (positive charges) or 2 (negative charges) in the table) for the separate charged species that dissociate from a neutral species, N_0, and have the common concentration c_0 but usually different mobilities and diffusion coefficients (the two-mobile situation when neither are immobile). Expressions for the impedance of the CJPNP model with arbitrary dissociation are given in Ref. 5, while one for the PNPA is presented in Eq. 6 of Ref. 7. The impedance expression for the full CJPNPA model is instantiated in the LEVMW computer program but is too lengthy to list here.

In the one-mobile situation (designated as 1 M in the table), the mobility of a positive or a negative species is set to zero, and only the other one reacts (and possibly adsorbs) at the electrodes. Fitting of the experimental data sets of [3,4] indicates that the one-mobile assumption is most appropriate for both sets and also for the ultra-pure water situation; see, however, the discussion below

of Table-1 data fit results. There the results of two different two-mobile type fits are included. The first is the ordinary two-mobile situation designated as 2 M, where the Π_m mobility-ratio parameter of the CJPNPA model is taken free to vary, and the second is the 2ME, where Π_m is held fixed at unity so the mobilities of both positive and negative charges are equal. Alternatively, when the value of Π_m is fixed at either a very large or very small value, effective one-mobile behavior is enforced in the PNP fitting model.

The 2ME two-mobile assumption with equal mobilities of the ions was made in both of the two earlier studies. The Duarte one assumed that the main mobile ions were the H^+ and OH^- species, while the Lenzi work did not identify the species of the mobile ions. It is highly unlikely that the mobilities of H^+ and OH^- are equal in water, but the situation is somewhat saved by the ambiguity that 2ME model fits differ only by small factors of some of their estimated parameters from the 1 M one-mobile ones [11], so they are practically interchangeable. In the Duarte and Lenzi fit results shown in rows 4 and 8 of Table 1, the 2ME parameter values are not adjusted to one-mobile ones since the differences are small and may be readily made from the results cited in Ref. 11, and their untransformed results may be directly compared to the full-dissociation 2 M fits listed in the table.

Two other significant differences are present, however. The Lenzi work of [3] involves a generalized PNP model that involves *two* fractional exponent terms to account for anomalous diffusion but a single reaction-rate parameter. In contrast, the Duarte analysis employs the combination of two fully blocking PNP models involving ordinary diffusion processes in parallel. Thus, only one diffusion constant (for both the positive and negative mobile species) is estimated in the Lenzi fit, but for the Duarte fit two diffusion coefficients (again the same for both the positive and negative mobile species of the two groups), putatively represent the dissociated water ions and an unidentified impurity molecule which dissociates completely to positive and negative ions of assumed equal mobilities.

It has already been mentioned that the PNP (or CJPNPA) designation here includes a high-frequency-limiting series resistance and a parallel capacitance (represented in specific form here by ρ_∞ and ε_∞, respectively). The resulting equivalent circuit is thus mostly comparable in form to the well-known and important simplest Randles circuit [12,Fig. 4.5.7], but the latter includes a resistor in series with the rest of the elements. It is, in fact, found that the addition of such a series resistor (ρ_s in specific form) to the full PNP model circuit is important in obtaining good fits of the data sets of [3 and 4]. The resulting composite model may be written as [(R∞ • CJPNPA)C∞] • Rs, where bullets denote series connections. For convenience, however, I will use just the designation CJPNPA here to include this full composite model and circuit. The only difference then between the CJPNA composite model fits and ones using the Randles circuit is the appearance of a finite-length Warburg response model in the latter and a PNP interface model in the former.

2.2.1. Duarte data [4] and fit results

Examination of the Duarte data of Fig. 1 shows that the three highest-frequency points are irregular, possibly arising from a change of measuring apparatus. The discrepancy is particularly evident in the real-part admittance curve of Fig. 1-b, but no data and fit results were included at the admittance level in the work of Ref. 4 so this problem was apparently unnoticed.. To eliminate the effect of this discrepancy, the last three high-frequency points were omitted from the data before fitting with the CJPNPA model in series with a resistivity parameter ρ_s, leading to the results of row-2 of Table 1. Of the 11 parameter values listed in columns 3-13, the six in columns 3,5,6,9,10, and 11 were free parameters of the fit and the remaining 5 were fixed or calculated from the other fit results.

All of the parameters in row-2 have already been mentioned except the mobility and diffusion coefficient ones of columns 12 and 13, and the important quantity $M_j \equiv L/(2L_{Dj})$ with j=1 or 2, where L_{D1} is the Debye length associated with a single mobile species, for example, protons in ultra-pure water, the 1 M one-mobile case. It is worth mentioning that for 1 M CJPNP models, the low-frequency-limiting dielectric constant associated with the PNP response is given by $\varepsilon_0 = [M_1 ctnh(M_1)]\varepsilon_\infty$ for full dissociation. Here, however, dissociation is small, and, as discussed on p. 495101-6 of [6], generation-recombination leads to essentially full mobilization of the fixed charges so that the above expression for ε_0 is replaced by one involving $M_2 \equiv \sqrt{2}M_1$, the 2 M two-mobile result. Here it leads, in the absence of anomalous diffusion, to the large value of ε_0 of about 2.88×10^6.

The ρ_s parameter is included here as part of the overall fit of the data in order to take account of the high-frequency rise of the real part of the admittance, Y', shown for both data sets in Fig. 1b. Such a rise is commonly seen in data involving mobile ions and is discussed for several different materials in Ref. 13. This rise is often found to be well fitted with either a Debye or Davidson-Cole model in parallel with the composite PNP model, but here the data sets do not include enough high-frequency points to yield significant estimates of the associated capacitances. When ρ_s is omitted, the fit-quality parameters $100S_F$ and 100PDRMS of row-2 increase to 5.84 and 10.0 respectively and those of row-6 increase to 3.66 and 5.69, respectively, both much poorer fits.

Comparison of relevant parameter values in rows-2 and 4 show that the Duarte work involved a separately estimated value of N_0 and, with the assumption of full dissociation, the same result for their c_0 estimate, one appreciably smaller than that directly estimated from the fit shown in row-2. Further, although the $\rho_\infty \simeq$ 1.77 *Mohm − cm* value of row-2 is appreciably larger than the value of 0.83 Mohm-cm for degassed pure water mentioned in Section 2.1, it is not greatly larger than the value mentioned there of about 1.3 Mohm-cm for ultra-pure water equilibrated with the atmosphere and stated to arise from CO_2 dissolved in the water.

The results of a 2 M two-mobile, fully dissociated fit of the Duarte data with the Π_m mobility-ratio parameter of the fitting model taken free to vary rather than fixed at unity are listed in row-3 of the table. It led to a Π_m estimate of 1163 ± 482, a very poorly defined quantity, indicating that the one-mobile assumption is more appropriate for this data set than is the two-mobile one. Nevertheless, it is valuable to compare the 2M-fit results for the mobility and diffusion estimates, with those of the 2ME Duarte fit of row 4. They are appreciably different, but the first values listed in columns 12 and 13 of row-3 are very close to those in the 1 M fit of row 2, so the second set of results in columns 12 and 13 are the ones of greatest uncertainty. A fit was also carried out that included the possibility of simultaneous electrode reactions for both the positive and negative 2 M charge carriers and it showed that only charge of one sign reacted there.

The results of the row-2 and row-3 fits indicate that the full dissociation assumption is inconsistent with the data. The comparison of the two fits also shows that the one-mobile mobility estimate of row-2 is appreciably smaller than that for ultra-pure water in row-1, again indicating that the mobile species present in the data is not likely to be that of protons. The estimate of the small c_0 concentration value of row-4 was used for both of the two groups of mobile positive and negative ions present in the Duarte fitting model but it is still appreciably larger than the value for ultra-pure water shown in row-1. In addition, the two row-4 mobile-ion diffusion coefficient estimates bracket the one of row-2, and the larger of the two estimates is somewhat less than that expected for ultra-pure water. All these results strongly indicate that the actual mobile ions dominating the behavior of the Duarte data set are most probably impurity ions, perhaps oxygen ones, and not protons. On this

assumption, the k_i parameter of row-2 of Table 1 is designated k_2 to specify the negative charge of the mobile reacting ions.

In normalized form, the value of the dimensionless Chang-Jaffé reaction-rate parameter corresponding to the k_2 reaction rate one of row-2, ρ_2 [5], is 0.009296, and it leads to a low-frequency-limiting plateau resistivity value of $(1 + \rho_2^{-1})\rho_\infty$ in the absence of anomalous diffusion [13]. Its numerical value is here about 1.926x10^8 Ω-cm. [14] includes in its Eq. 7 an explicit expression for the impedance of the CJPNP model with full or arbitrary dissociation. In Ref. 4, which indeed considers ordinary rather than anomalous diffusion, two boundary condition quantities, s_1 and s_2, are defined and evaluated from the data fit. According to the model used they may be related to conductivity quantities associated with partial blocking of the ions as they react at the electrodes. Unfortunately, it appears that the inverses of the resulting conductivities are very far from being close to the limiting Chang-Jaffé plateau value cited above. In summary, it appears that the Duarte fitting model is indeed reasonably successful in explaining the low-frequency rise in the real part of the impedance, but it does not lead to either parameter estimates associated with ultra-pure water or to those following from the full CJPNPA-model fit of row 2.

2.2.2. Lenzi data [3] and fit results

Unlike the fitting model of Duarte [4], the generalized PNP model used in the Lenzi work [3], which will be described here by the acronym GEPNPA, involves a fractional-diffusion integro-differential equation of distributed order and thus directly includes the possibility of anomalous diffusion [3]. In Ref. 4 the Lenzi approach is characterized as "equivalent to a constant phase element masked by a kernel present in the boundary conditions."

In fact, in its present application to fitting "pure" water data the GEPNPA involves *two* CPE-like fractional-exponent functions, although it is not made clear exactly how they appear in the tanh functions present in the Lenzi expression for the impedance [3]. Only one CPE term appears, however, in the anomalous-diffusion CJPNPA model and none for the ordinary diffusion process inherent in the simpler CJPNP one. Thus the GEPNPA Lenzi model is intrinsically more general than even the CJPNPA one, and it led to a better fit of the water data than did the Duarte approach, but its theoretical response has not so far been compared and fitted by a CJPNPA model or by any other earlier PNP models.

Thus it has not yet been established that the GEPNPA model is appreciably different from or better than the CJPNPA for the data sets that it has been used to fit in the last several years. This lack is remedied somewhat, however, in the present work since the same water data fitted by the GEPNPA model in [3} has been fitted here by the CJPNPA one in series with the ρ_s resistivity parameter discussed in the section above. No such parameter is included in the GEPNPA model, however, although the water data fitted in [3] shows, as in Fig. 1b, a small high-frequency rise in the real part of its admittance response.

Rows 6 and 8 of Table 1 compare such a composite CJPNPA-model fit of the Lenzi data with that of the GEPNPA of [3]. The question mark in the ψ_p column of row 8 is present because two negative fractional exponents are listed from the GEPNPA fit but if one adds the negative exponent of the one of larger magnitude to unity one obtains 0.76, close to the value of 0.78 of the row-6 fit. Neither of the diffusion coefficient estimates of rows 6 and 8 is as large as the likely protonic value of row 5, again indicating that the principal mobile charge species of the "pure" water is not protonic but, as with the Duarte results, it is likely that of an impurity species. Finally, the question mark after the value in the k_i column for row-8 is there because although this value has the dimensions of a reaction rate, it is not clear that it should be directly compared with the CJ estimate of row-6, one that is several magnitudes smaller and probably more physically realistic. Again a CJPNPA 2 M

fit of the Lenzi data set with free reaction-rate parameters for the mobile charges of both signs was not successful, indicating that charges of one sign react and those of the other sign are completely blocked.

When the mobility ratio Π_m is not fixed at unity, as it would be for a fully dissociated CJPNPA fit of the Lenzi data set, but when it is allowed to be free with a starting value equal to the two-mobile result found for the Duarte data, the 2 M fit results of row-7 are different from those of the Duarte fit of row-3. Instead, the fit estimate of Π_m of about 33.6 ± 7.9 is poorly defined but still appreciably better defined and much smaller than the corresponding Duarte one. Further, it is interesting that the values of the bottom column-12 and -13 mobility and diffusion coefficients of row-7 are rather close to those obtained from the 2ME Lenzi fit of row 8, while the two top values agree less well with the comparable results of row 6. Nevertheless, the c_0 estimate of row-8, obtained directly from the GEPNPA model fit, is appreciably less than the comparable values of rows 6 and 7. Although the 2 M fit results of row-7 are closer to two-mobile response with equal mobilities than that of row 3, the present results indicate that a 1 M fit is both better and more appropriate for the Lenzi as well as for the Duarte water data sets.

3. Conclusions

Although the Duarte, Lenzi, and CJPNPA models all take account of the low-frequency rise in the real part of the impedance apparent for the two data sets shown in Fig. 1, only the CJPNPA one also models the high frequency rise in the real part of the admittance shown in this figure, and it leads to appreciably better fits of the two water data sets than do the other two approaches. Further, they generally involve more free or independently estimated parameters than does the CJPNPA, and no results are included for their goodness-of-fit and free-parameter uncertainty estimates. Thus Occam's razor suggests that the CJPNPA model is more physically appropriate and preferable to the other approaches.

The present work derives likely immittance responses for ultra-pure water and compares them with good CJPNPA fits of the "pure" water data sets of Refs. 3 and 4 and with those obtained by the authors of these papers, where different fitting models were employed. The "pure" water data sets investigated by impedance spectroscopy in these works and here are evidently ones that have equilibrated with the atmosphere and no longer exhibit ultra-pure water behavior. The present results quantify the difference between these two such data sets and also show how they differ from the expected response of ultra-pure water. The quantitative differences found make it clear that the mobile ion behavior of these water samples is dominated by that of impurity ions and not by protonic conduction. Comparison of CJPNPA-model fits of the data sets of Refs. 3 and 4 with only ions of a single sign taken mobile and with ones in which both positive and negative ions are allowed to be mobile shows that the one-mobile situation is most likely and that the mobile ions are not protons but possibly oxygen ones.

Finally, in a contemporary review paper [15] of the present author about the use of PNP models for IS data analysis, the work of Refs. 3 and 4 has been mentioned and briefly discussed and the need for further model fitting and analysis of these results pointed out. That need is addressed here. In the review, a comprehensive discussion is provided of past and present usage of PNP models, such as the CJPNPA model employed in the present work. There, responses are demonstrated for all four immittance levels and the wide applicability of this model is illustrated by citing its prior use to fit unsupported IS data sets for a variety of different materials and by showing how it can well fit data previously analyzed by other

models such as the Davidson-Cole one and data possibly involving finite-length Warburg response such as that of the important Randles circuit [12]. As demonstrated herein, a main virtue of the CJPNPA fitting model is that unlike most other models it leads to estimates of such important parameters as ionic concentrations and mobilities and reaction-rate and adsorption ones.

Acknowledgments

References

[1] E. Tajkhorshid, P. Nollert, M.O. Jensen, L.J.W. Miercke, J. O'Connell, R.M. Stroud, K. Schulten, Science 296 (2002) 525–530.
[2] J.R. Macdonald, J. Chem. Phys 102 (1995) 6241–6250.
[3] E.K. Lenzi, P.R.G. Fernandes, T. Petrucci, H. Mukai, H.V. Ribeiro, Phys. Rev 84 (2011) 041128–041133.
[4] A.R. Duarte, F. Batalioto, G. Barbero, A.M.F. Neto, J. Phys. Chem. B 117 (2013) 2985–2991.
[5] J.R. Macdonald, D.R. Franceschetti, J. Chem. Phys 68 (1978) 1614–1637.
[6] J.R. Macdonald, J. Phys.: Condens. Matter 22 (2010) 495101–495116, The incorrect Eq. (A-12) in this work is corrected in Ref. 7 herein.
[7] J.R. Macdonald, L.R. Evangelista, E.K. Lenzi, G. Barbero, J. Phys. Chem. C 115 (2011), 7648–7648.
[8] H. Chang, G. Jaffé, J. Chem. Phys 20 (1952) 1071–1077.
[9] J.R. Macdonald, L.D. Potter Jr., Solid State Ionics 23 (1987) 61–79;
J.R. Macdonald, J. Computational Phys 157 (2000) 280–301;
The newest WINDOWS version, LEVMW, of the comprehensive LEVM fitting and inversion program may be downloaded at no cost by accessing http://jrossmacdonald.com. It includes an extensive manual and executable and full source code.
[10] C.J.T. de Grotthuss, Ann. Chem 58 (1806) 54–73.
[11] J.R. Macdonald, J. Phys.: Condens. Matter 24 (2012) 175004–176015.
[12] *Impedance Spectroscopy- Theory, Experiment, and Applications*, Second Edition, E. Barsoukov and J. R. Macdonald, Eds.; John Wiley & Sons: New Jersey, 2005. See the Randles circuit diagrams on pp. 308, 446, and 447.
[13] J.R. Macdonald, M.M. Ahmad, J. Phys.: Condens. Matter 19 (2007) 046215–046228.
[14] J.R. Macdonald, J. Phys. Chem. A 115 (2011) 13370–13380.
[15] J.R. Macdonald, J. Phys. Chem. C 117 (2013) 23433–23458.